

---

# CEOS.fr Project Presentation

---

The overall objective of the CEOS.fr project is to take a significant step towards improving the engineering capabilities for assessing concrete structure crack patterns and predicting the patterns expected under anticipated design conditions. Crack control is crucial to ensure serviceability (durability and sustainability) throughout the working life of concrete structures. Current engineering practice provides some recommendations for limiting concrete cracking, with crack width and spacing control based on formulae supported by empirical data from test beams (small-sized test specimens) submitted to bending moments or tensile force. While the current codes are considered to be reasonably representative for these load cases, previous results indicate that these formulae are not fully consistent when applied to shear walls or massive structures. Hence, within the CEOS.fr national research project, several experiments on massive concrete beams were conducted to improve the knowledge of cracking phenomena, by coupling numerical modeling and experimental approaches.

## 1.1. CEOS.fr work program

The CEOS.fr program includes three work areas that are relevant for the control of cracking:

- *monotonic loads*: the purpose of which is to calibrate the available methods for predicting crack patterns and related strains under tensile or bending conditions;

– *thermo-hydro-mechanical (THM) behavior*: the purpose of which is to account for the effects on cracking of strains induced by early age behavior, shrinkage and the consequences of long-term drying, with due consideration given to boundary conditions;

– *seismic and cyclic loads*: the purpose of which is to consider the seismically induced crack patterns in shear walls, either during or after the seismic event, taking into account the cumulative damaging effects of all loads.

The three aforementioned work areas were studied according to the following three approaches:

– *testing*: implementing tests on large-scale specimens (full scale, 1/3 scale ties and beams, 1/3 scale shear walls) with well-identified boundary conditions and accurate crack pattern monitoring;

– *modeling*: applying the existing numerical models and developing specific models compatible with engineering issues;

– *engineering*: developing design rules from test results and numerical simulations with the aim of establishing *guidelines for the control of cracking phenomena in reinforced concrete structures*.

### 1.2. Testing

Few experimental results which relate to large or massive structures are found in the literature. Hence, four types of specific tests were performed under the framework of the CEOS.fr project, as described in the following section.

All test block specimens were comprehensively monitored to locate and follow crack propagation and to measure crack spacing and crack widths. Digital Image Correlation (DIC) was specifically used to measure crack widths on the whole surface of the test specimens (see section 11.5 for details).

#### 1.2.1. Tests on prismatic full-scale blocks

##### 1.2.1.1. Tests on free strain blocks

Figure 1.1 depicts the basis of the seven full-scale blocks (dimensions 6.10 m × 1.60 m × 0.80 m), designated RL1 to RL7. These blocks were

constructed according to specifications summarized in Table 1.1. Two identical reference blocks, RL1 and RL6, were constructed from C50/60 class concrete and 16 HA Ø 32 reinforcing bars. The other individual blocks were produced using the same criteria, but with one feature changed compared to the reference blocks, either concrete grade, concrete cover, reinforcing bar diameter or reinforcement ratio (Table 1.1). The average reinforcement ratio was approximately 1%, which is representative of such structures.



**Figure 1.1.** *RL block with free deformations (Top) and its reinforcement (Bottom)*

Block/Beam	Specificity	Concrete cover (mm)	Cement	Concrete class	Reinforcement bars HA (top)
RL1 RL6	Reference beams	50	CEM1 52,5N CE CP2 NF	C50/60	16 Ø 32
RL2	Minimum percentage of reinforcement	50	CEM1 52,5N CE CP2 NF	C50/60	4 Ø 32
RL3	Increased bar diameter	50	CEM1 52,5N CE CP2 NF	C50/60	10 Ø 40
RL4	Increased concrete cover	70	CEM1 52,5N CE CP2 NF	C50/60	Ø 32
RL5	Reduced concrete resistance	50	CEM1 52,5N CE CP2 NF	C30/37	16 Ø 32
RL7	Addition of two inclusion vertical cables	50	CEM1 52,5N CE CP2 NF	C50/60	16 Ø 32

**Table 1.1. Characteristics of RL blocks**

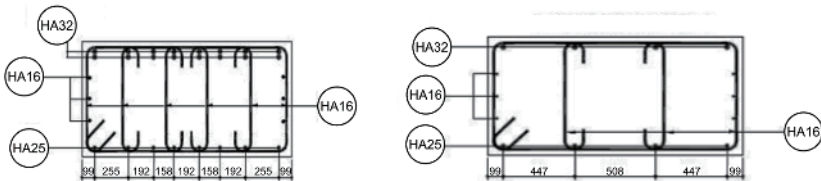


**Figure 1.2. Reinforcement bars HA of block cross-sections: RL1, RL5, RL6 and RL7 (left figure) and RL2 (right figure)**

Post casting, the seven blocks were freely matured for a period of at least 4 weeks, with limited protection provided against major weather conditions. Following this period, each block was moved onto the test bench and secured with four prestressing bars used to hold the block in place. The block was then submitted to a monotonic bending load by two rows of  $4 \times 1,000$  kN capacity jacks, 6,000 mm spaced and symmetrically positioned under the central part of the beam (Figure 1.3).

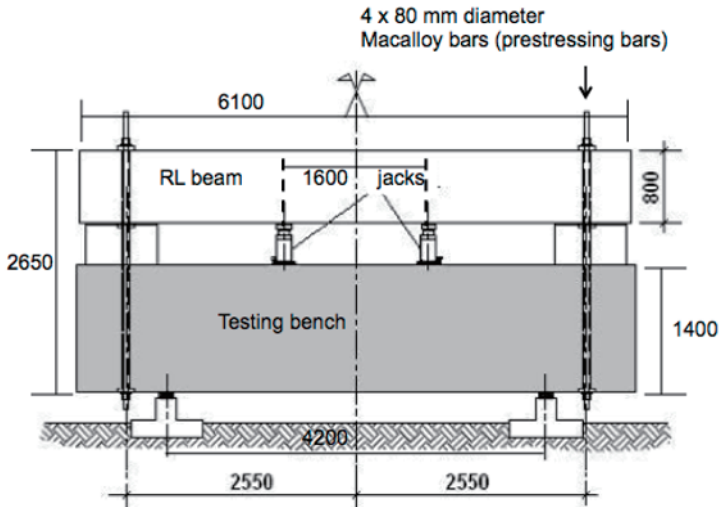


**Figure 1.3.** Specification and principle of bending test for RL block (beam)

Flexural tests were then performed at incremental steps of 150 kN, up to a maximum load varying from 2,000 to 2,500 kN depending on the beam. The maximum bending moment applied varied from 1,600 to 2,000 kNm, except for RL2. This approach was taken to ensure that the crack pattern was completely stabilized for each beam and, hence, that the Service Limit State (SLS) is fully addressed.

The top reinforcement bars support a maximum stress of approximately 400 MPa (EC2 and MC2010), which is the theoretical steel stress at the concrete crack.

With the exception of RL2, which was close to failure, resulting from the minimum percentage of reinforcement used, block failure did not occur.

To confirm crack pattern evolution with bending load, specific DIC procedures were developed, which provided full measurement of the crack width evolution and crack spacing with the applied bending load.

The resultant DIC surface measurements were correlated with internal measurements of the temperature evolution inside the specimen blocks (temperature gradient), overall and local strain evolution and rebar stress. Hence, to support this approach, at least three surfaces are instrumented,

positioned centrally in each block. The analysis of the resultant data has led to a greater understanding of the cracking phenomena associated with the most significant cracks (see Figure 1.4):

- the crack pattern is largely dependent on the early age of the block. In massive blocks, high temperature levels are reached in the core. Temperature gradients can lead to early cracking on the block surface after formwork removal or at the block core with restrained shrinkage due to the reinforcement layers;

- surface cracks generally close during the maturing phase and do not influence the crack pattern obtained under mechanical loading;

- core cracks may influence the crack pattern obtained under mechanical loading as crack spacing and crack widths are larger;

- for massive structures, where reinforcement bar cover is more significant, the concrete crack widths are generally greater. Section 4.2 presents an approach which gives more details on how this test feature is taken into account.

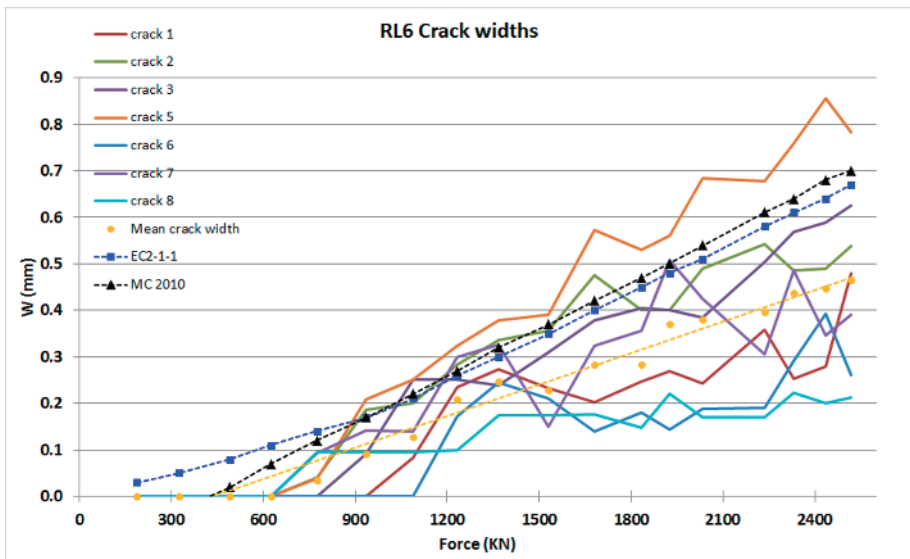


**Figure 1.4.** Crack evolution on prismatic beams tested in bending: a comparison between the test results from several cracks (solid lines) and the comparable code-based provisions (dashed lines) for full scale beam RL6

In addition, tensile resistance of thick elements is lower than the tensile strength calculated in accordance with EC2-1-1 ( $f_{ct, 0.05} = 0.7 f_{ctm}$ ).

$$f_{ct, 0.05} \approx 0.5 f_{ctm}$$

This relationship is due to the 3D stress distribution in the thick element cross-section and the associated scale effect, since the cross-section of the massive beam is significantly larger than the cross-section of the specimens tested in the laboratory, used to calibrate the EC2-1 formula. Hence, the actual  $f_{ct, 0.05}$  value is more likely to be reached in a massive structure.

NOTE.– Section 11.5 of the Guidelines gives more details on the measurement system used for the test specimen blocks.

### 1.2.1.2. Tests on blocks subjected to restrained shrinkage

The three concrete blocks RG8, RG9 and RG10 were constructed using three parts (Figure 1.5):

- a central prismatic block ( $6 \text{ m} \times 0.50 \text{ m} \times 0.80 \text{ m}$ ), which comprises the block;
- two head blocks ( $0.9 \text{ m} \times 2.2 \text{ m} \times 0.9 \text{ m}$ );
- two steel struts, which restrain strains to induce cracks in the block.

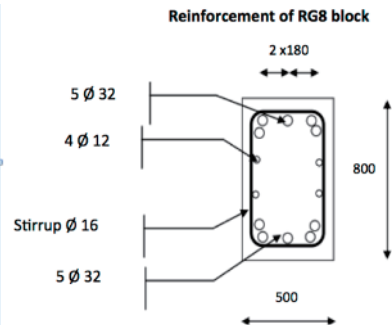


**Figure 1.5.** RG8 block with restrained shrinkage (I-shaped beam and steel struts)

During the RG block-maturing phase, the following were measured: overall strains, local strains and temperatures on the block surface, the block core and along the rebar. Average strut forces were also measured during the test. The RG block local concrete strains were compared with the strains

measured in the concrete specimens cast on site (freely matured test specimens and quasi-adiabatic test specimens) to assess the restrained concrete shrinkage.

Block/Beam	Specifics	Cover (mm)	Cement	Concrete class	Reinforcement ratio
RG8	Reference beam	50	CEM I 52,5N CE CP2 NF	C50/60	2%
RG9	Reduced reinforcement	50	CEM I 52,5N CE CP2 NF	C50/60	0.6%
RG10	Increased cover	70	CEM I 52,5N CE CP2 NF	C50/60	2%

**Table 1.2.** *RG block characteristics*

These changes demonstrate early age cracking due to THM effects, which result from the temperature increase during the concrete setting, the temperature decrease and the restrained shrinkage. During the tests, of a 400-hour duration, three to four cracks appeared in the central beam sections, despite the fact that the stabilized cracking stage was never reached. Cracks were detected by the measurement system (strain gauges, Linear Variable Differential Transformer (LVDT) and fiber sensors).

The main difficulty in carrying out this test is to forecast where cracks will occur in order to implement the sensors at the right place. However, the transfer of shear forces between concrete and steel bars in the vicinity of cracks can be derived from measurements.

The maximum and minimum crack width tests result from RG8 (with 2% reinforcement), maximum crack width 107  $\mu\text{m}$ , was less than that obtained from RG9 (with 0.6% reinforcement), maximum crack width 126  $\mu\text{m}$ .

### 1.2.1.3. *Main experimental outputs of massive test blocks*

The most significant finding from the CEOS.fr project is an improved understanding of the THM effects for early age concrete. At an early age, the massive elements are submitted to non-uniform strains, which may induce



cracking at this stage. This effect is unavoidable in practice and is generated by:

- temperature gradients between the core and the surface of the massive element;
- internal strains generated due to the temperature profile, shrinkage and creep.

In addition, the assessment and interpretation of the test results for massive elements has improved the understanding of the influence of two phenomena: 3D effects, as the massive elements are always submitted to 3D non-uniform strains, and probabilistic scale effects.

To explain the effects seen on massive structures, it is necessary to assume that the mean tensile strength is reduced compared with the split test and that the stress distribution is non-uniform, mainly due to the probabilistic scale effect (referred to in MC2010 clause 7.12.5.4): the volume of concrete submitted to high tensile stress is larger when compared to that submitted to tensile stresses in a specimen under tensile test (see NF EN 12390-6 split tensile test). In this example, the likelihood that the tensile strength value  $f_{ct,0.5}$  is reached for massive structures is much greater than that in a laboratory test specimen.

The probabilistic scale effect can be simulated by using the Weibull theory, and the weak value of the tensile strength can be mainly explained by the use of a simplified approach based on this theory (see section 2.2).



**Figure 1.6.** *RL1- 1/3 scale beam under reinforcement*

### 1.2.2. Tests on 1/3-scale beams

Six 1/3-scale blocks ( $1.90 \text{ m} \times 0.25 \text{ m} \times 0.44 \text{ m}$ ) were manufactured in accordance with the specifications given in Table 1.3.

Beam1/3	Specifics	Cover (mm)	Concrete class	Reinforcement bars (top)	Stirrup spacing (mm)
A	Standard concrete	15	C 50/60	16 Ø 10	100
B1 – B2	First use of micro concrete B	15	C 50/60 micro concrete	16 Ø 10	100
C	Reduced number of rebars	15	C 50/60 micro concrete	8 Ø 14	100
D1 –D2	Stirrup spacing increased	15	C 50/60 micro concrete	16 Ø 10	144

**Table 1.3.** 1/3-scale block characteristics

The purpose of these tests was to highlight the scale effect on the behavior of the beam when compared with the full-scale prismatic blocks, and to verify its validity for structures designed in accordance with EC2, which relates to the crack width and spacing assessment.

Each 1/3-scale beam, with free deformations, is subjected to monotonic loading adapted from the full-scale beam flexural tests. These tests were conducted in a step-by-step manner. Each of the 18 load steps is applied by two jacks at a spacing of 500 mm, up to a maximum load of 234 kN (Figure 1.6). In practice, a pre-load is applied to the 1/3-scale beams to calibrate the load system. Each load step was scaled according to the crack width measurement and crack spacing.

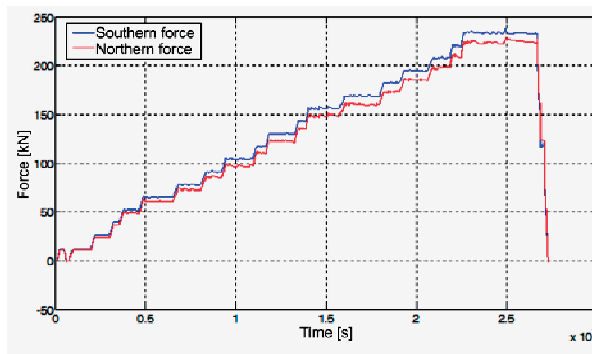


**Figure 1.7.** 1/3 scale beams load path

Measurement	Sensor	Number	U.M.	Location	Comments
Temperature	PT 100	2	°C	Concrete (internal)	Embedded
Force	Transducer	2	kN	Central	Upward vertical direction
Strain (+ temperature)	Vibrating wire strain gauge (VWSG)	4	$\mu\text{def}$	Concrete (internal)	Longitudinal direction
Strain	Gauge	3	$\mu\text{def}$	Upper edge	Longitudinal direction
Strain	Sensor with Fiber Bragg Grating (FBG)	4	$\mu\text{def}$	Welded on rebars	Longitudinal direction
Displacement	Long base optical extensometer (LVDT)	8	mm	Upper and lower edge	Vertical direction

**Table 1.4.** 1/3-scale beam test measurements

Figure 1.8 gives the location of the sensors on the 1/3 scale beam B2: temperature probes PT 100, strain gauges glued to the upper level rebars and Vibrating Wire Strain Gauge (VWSG) embedded within the concrete.

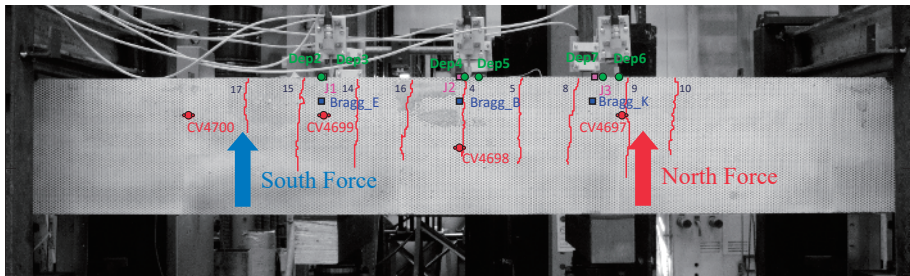


**Figure 1.8.** Sensor location on the painted side of the 1/3 scale tested beam and crack pattern detected at the test final load using digital image correlation (Fiber Bragg Grating (FBG)), Vibrating Wire Strain Gauge (quoted CV), temperature sensors (Pt 100), displacement sensors (Dep)

For 1/3-scale beams, the test results demonstrate that the mean crack spacing and widths at the stabilized cracking stage are consistent with the crack spacing and width calculated using the MC2010 formulae. Note that the beam size used corresponds to test results and on-site observations used to establish the EC2 and MC2010.

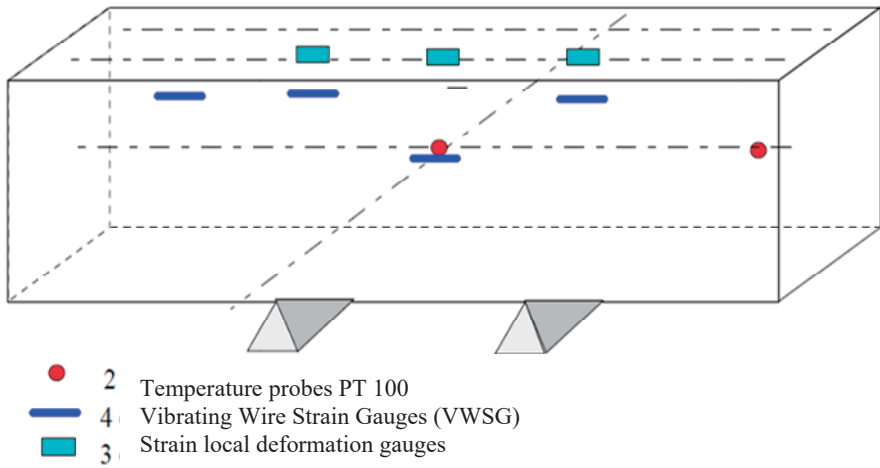


Figure 1.9. B2 tested 1/3-scale beam displaying the location of various sensors

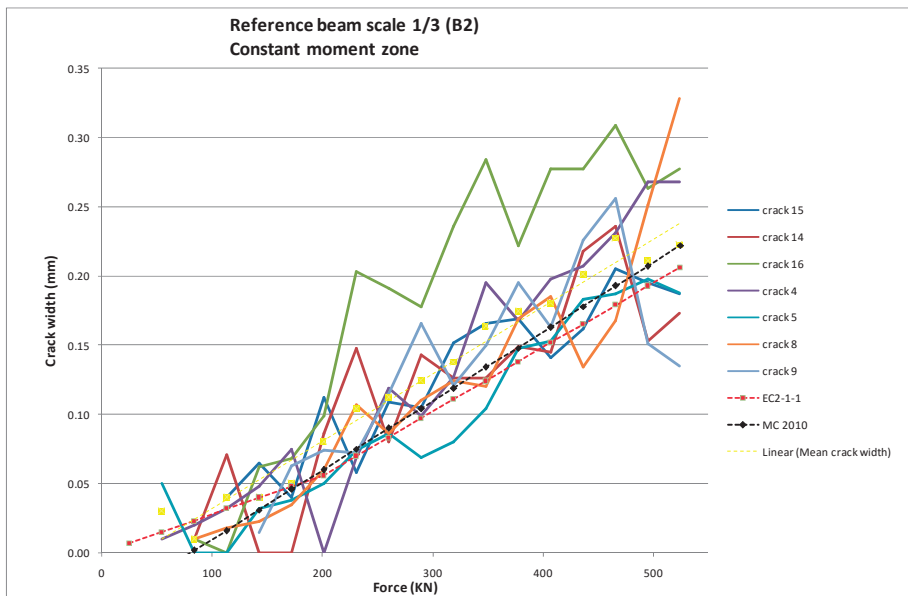


Figure 1.10. Crack evolution on prismatic beams tested in bending: a comparison between the test results from several cracks (solid lines) and the comparable code-based provisions (dashed lines) for a 1/3-scale beam

### 1.2.3. Tests on 1/3-scale shear walls

Four 1/3-scale shear walls (height = 1.05 m, length = 4.2 m, thickness = 0.15 m), designated SHW1 to SHW4, were manufactured according to the specifications summarized in Table 1.5. In addition to the similitude rules, the design of these test specimens was driven by two conditions:

- to accurately reproduce reinforced thick shear walls representative of industrial structures;
- to adapt the availability of the testing means, the capacity of jacks of the testing bench being limited to 4,500 kN.

As presented in Table 1.5, the walls differ from each other due to either the type of concrete or the reinforcement mesh.

The mock-up was installed in a rigid steel frame, thereby avoiding any large reactions on the test slab specimen. This also enables improved control of applied forces and boundary conditions. The load actuator was installed between the upper beam and the steel frame.

Shear wall	Concrete class	Reinforcement bars	Load type
SHW1	C25/30	HA10 – 100 mm × 100 mm	Reversing cyclic loading
SHW2	C40/50	HA10 – 100 mm × 100 mm	Reversing cyclic loading
SHW3 reference wall	C40/50	HA10 – 100 mm × 100 mm	Non-reversing loading
SHW4	C40/50	HA8 – 80 mm × 80 mm	Reversing cyclic loading

**Table 1.5.** Characteristics of 1/3 scale shear walls

To obtain the most even shear force spreading possible, two highly reinforced horizontal beams were horizontally connected to the top and bottom of the shear wall. As the walls were designed without flanges, vertical steel bars were added to reinforce both edges to control the crack opening due to the induced bending effect (Figure 1.10).

The shear walls given in Table 1.5 were tested incrementally until failure. Three of the walls were subjected to horizontal reversing load applied in a series of three cycles, with a  $\pm 300$  kN increasing load step. The SHW3 reference wall specimen was tested under a non-reversing load applied in a single “push” direction, as shown in Figure 1.10.



**Figure 1.11.** Shear wall specimen SHW3 (left figure) and shear wall reinforcement (right figure)

### Envelop curves

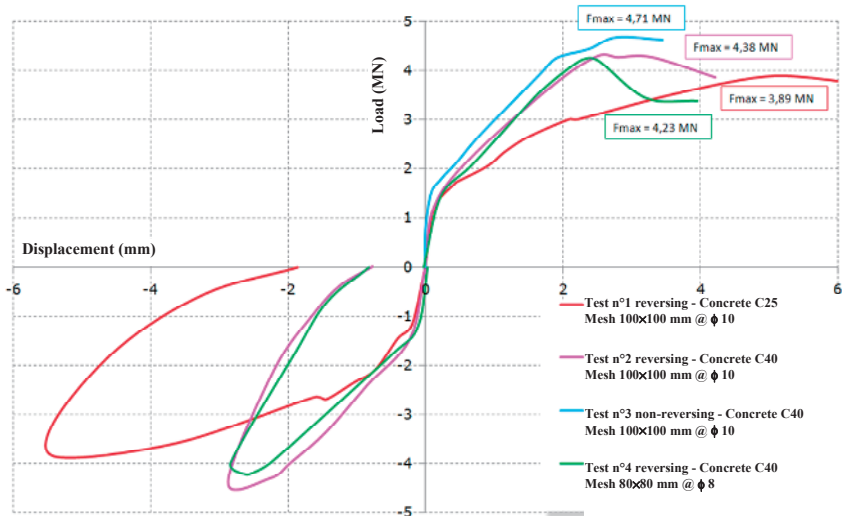


**Figure 1.12.** Comparison of force-displacement envelope curves related to the four SHW tests

During these tests, the ultimate strength is not reached through rupture in the central zone, but by sliding along the plane between the wall and the upper beam, extended by an inclined plane joining the horizontal bottom support. This effect has been reproduced across all the four walls.

### 1.2.3.1. Non-reversing loading test

During the non-reversing loading test, the influence of the following factors has been assessed, with the spacing  $S_r$  between cracks compared to EC2 and MC2010-formulae-based results. In addition to this approach, other results from the SAFE experiment (ISPRA) have been re-analyzed, especially at Ultimate Limit State (ULS), with the CEOS.fr outcomes demonstrating consistent agreement with the SAFE results.

#### 1.2.3.1.1. Concrete cover

The results of the shear wall tests show that it is advisable to use, for calculation purposes, either the cover for each rebar layer or the mean value of the two covers in both directions. Of the two approaches, the second (mean value) solution is considered to be simpler to apply.

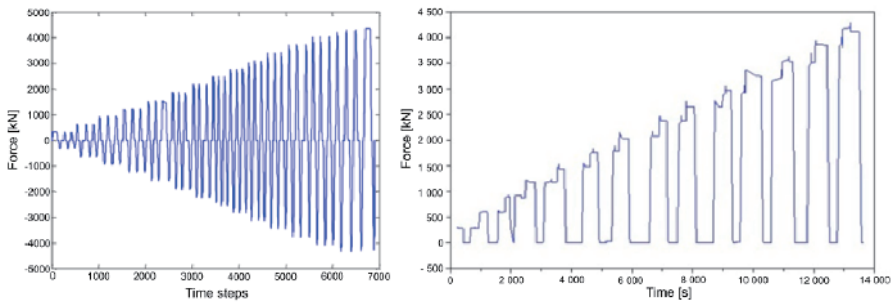


**Figure 1.13.** Load path of specimens SHW1, SHW2, SHW4 (left) and SHW3 (right)

#### 1.2.3.1.2. Angle $\theta$

Angle  $\theta$  is the angle between the reinforcement in the horizontal direction and the direction of the crack determined by the principal tensile stress. If the reinforcement layers are in accordance with the optimized ratio between horizontal and vertical reinforcement, an error in angle  $\theta$  assessment does

not result in a significant error in the assessment of crack spacing and crack width.

#### 1.2.3.1.3. Structural tensile resistance of concrete $f_{ctm}$

The test results show that the mean structural tensile resistance  $f_{ctm}$  is 40% less than the theoretical value of  $f_{ctm}$  when the first crack occurs. This reduction is due to the 3D effects for massive elements, resulting in stress variations across the section.

Scale effects between  $f_{ctm}$  measured on specimens under laboratory conditions and  $f_{ctm}$  results observed on the large concrete volume of the tested shear walls are also a factor which contributes to reducing  $f_{ctm}$  in shear wall tests. In addition to these scale effects, the effect of concrete struts working in compression may also decrease the tensile strength.

The value of the compressive strength  $f_{cm}$  demonstrates some impact (approximately 20% between SHW1 and SHW2 shear wall tests n°1 and 2, respectively) on  $S_r$  value and cannot be discounted, although it should be noted that both EC2-1 and MC2010 do not take this parameter into account.

The crack width  $w_d$  has been measured for comparison with EC2 and MC2010 formulae.

#### 1.2.3.1.4. Influence of reinforcement ratio

For test SHW4, the overall reinforcement ratio falls from 1% to 0.8%, while  $S_r$  is seen to increase by up to 22%. However, the application of the EC2 and MC2010 formulae gives a reduction in  $S_r$ , due to the formulae being based on the effective area. This approach appears to be unsuitable for the calculation of  $S_r$  (Figure 1.14).

#### 1.2.3.2. Comparison of reversing and non-reversing loading tests

$\theta$  varies by approximately 10% depending on the “pushing” direction applied during the test, and is not dependent on  $f_{ct}$ .

The test results show that cracks close during the reversing load test, when the load is approximately zero, and that cracks do not close during non-reversing load tests. Crack width increases with the load during the cyclic testing.



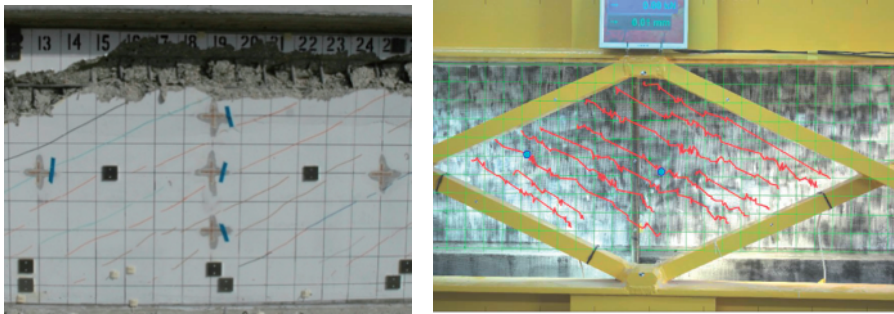






**Figure 1.14.** Damaged central part of shear wall SHW3 at collapse, under non-reversing loading (left figure) – reconstruction of crack pattern with DIC on the opposite side (right figure)

### 1.2.4. Tests on ties

Nine large ties, constructed from concrete C40/50 in accordance with the requirements given in the NF EN 206-1 standard, were tested under laboratory conditions with various sizes and types of reinforcement used as described in Table 1.6.

Type of tie	Number of ties	Dimensions	Reinforcement
	2	135 × 135 × 3,200 mm	1 rebar $\Phi 25$
	2	170 × 170 × 3,00 mm	1 rebar $\Phi 40$
	3	355 × 355 × 3,200 mm	4 rebars $\Phi 25$ One tie with stirrups $\Phi 10@200$ mm
	2	355 × 355 × 3,200 mm	8 rebars $\Phi 16$ with cross bracing $\Phi 8$

**Table 1.6.** Tie characteristics

#### 1.2.4.1. One rebar concrete tie test

For each bar diameter, two types of loading were applied:

– direct tension loading: concrete ties were loaded at a slow speed, with the crack pattern recorded for each loading stage ( $R_e/4$ ,  $R_e/2$ ,  $3/4R_e$  and  $R_e$ ,

elastic limit). Tests were performed up to the maximum rebar extension allowed by the stroke of the jacks monitoring the loading;

– cyclic tension loading: these tests were performed using the same methodology as for the direct tension tests. In addition, four loading–unloading cycles were performed at each of the two post-yielding stages, corresponding to bar elongations equal to 25 mm and 50 mm, respectively.

#### 1.2.4.2. *Four or eight rebar concrete tie tests*

Only direct tensile tests were performed for ties with four or eight rebars, under the same conditions as described in section 1.2.4.1.

#### 1.2.4.3. *Measurements*

The bar and concrete elongations of the tie were recorded with sensors installed at both ends of the specimen. The crack pattern (crack location and width) was recorded at each loading stage. For the latter, two types of crack measurement apparatus were used: micro-sensors and a microscope linked to a screen [MER 14].

#### 1.2.4.4. *Main outputs from tie test results*

##### *Tensile strength*

The results from tie tests demonstrate that the first cracks appear in the concrete cross-section under a lower tension load than predicted by the conventional tensile stress  $0.7 f_{ctj}$ : e.g. values of 1 or 2 MPa compared to the 3 MPa predicted by the formulae and the even higher values measured on cylinders.

##### *Crack spacing*

The maximum spacing,  $S_{r,max}$ , measured between stabilized cracks is less than that predicted by the EC2 – expression [7.11] applied to large ties, which significantly overestimates this spacing. The maximum spacing calculated from the MC2010 – expression 7.6.4 appears to provide spacing values with a better agreement with the test results, although still higher, as given in Table 1.7.

Test results related to crack spacing measured on tie specimens have been integrated into the statistical study giving the crack spacing for a tie in tension (see section 3.3).

Tie	Diameter rebar (mm)	Number of rebars	Experimental			Theoretical according to MC2010 and EC2-1	
			Average crack spacing (mm)	Standard deviation crack spacing (mm)	Characteristic crack spacing (mm)	2ls, max MC2010 (mm)	Sr, max EC2-1 (mm)
4	40	1	178	67	289	392	426
5	40	1	178	65	284	392	426
9	25	1	168	58	264	360	430
10	25	1	152	53	239	360	430
1	25	4	200	80	331	590	664
2	25	4	200	78	329	590	664
3	25	4	246	77	373	590	664
4	16	8	160	59	257	437	534
5	16	8	188	79	318	437	534

**Table 1.7.** Comparison of crack spacing between test measurements and values calculated from EC2 and MC2010

### Crack width

The maximum crack width measured is close to the value calculated both from EC2-1 and MC2010 (Figures 1.15 and 1.16), which suggests that the relative mean strain value might be underestimated by these codes.

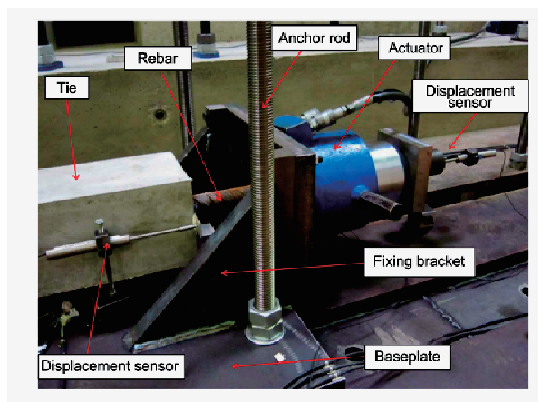


**Figure 1.15.** Jack and displacement sensor

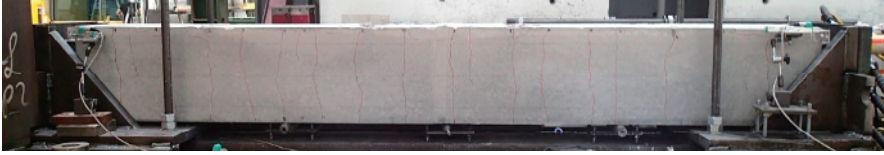


**Figure 1.16.** Tie with eight reinforcement bars at crack saturation stage

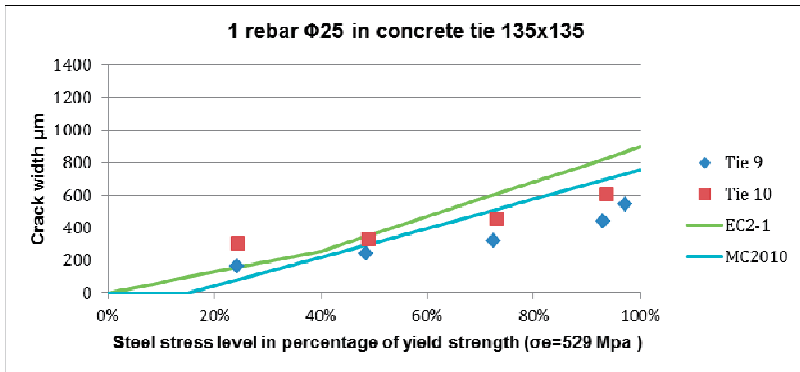


**Figure 1.17.** Crack widths compared between test results and EC2/MC2010 calculations for one rebar tested ties 9 and 10

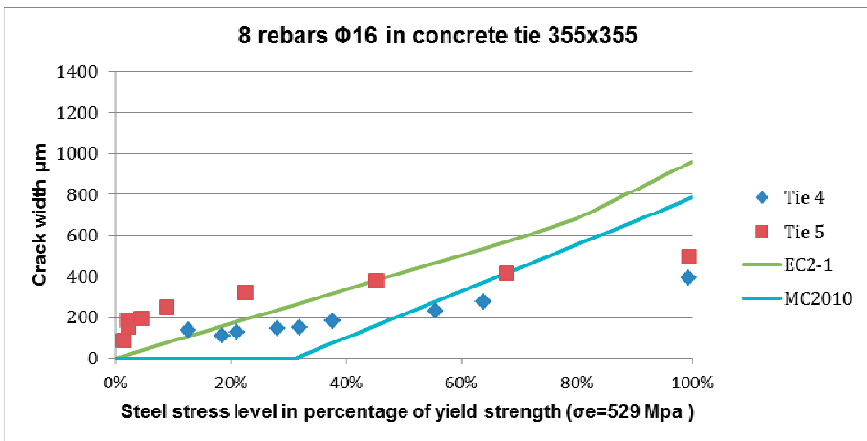


**Figure 1.18.** Crack widths compared between test results and EC2/MC2010 calculations for eight rebar tested ties 4 and 5

### 1.3. Modeling and simulation

Numerical modeling played a key role in the interpretation of test result data obtained from the cracking of massive elements at an early age and 1/3 scale shear wall tests. Comparison of model numerical results with the experimental data obtained from instrumentation has provided an improved understanding of the physical phenomena due to scale effects and THM effects in massive structures [BUF 16]. As a result, it was possible to use modeling and other simulation tools to extend the range of the experimental program results, through numerical “virtual” modeling of the physical processes.

A considerable number of studies have been performed using models and modeling. Several actions were launched in parallel: benchmarking of the basis of existing experimental results, either from the CEOS.fr project experiments or the established dedicated research programs, such as MEFISTO (see section 1.3.1).

These benchmarking actions helped as a first phase to test the existing models and as a second phase to improve the performance of these models or to develop new operational models for the analysis of the experiments performed. Finally, in addition to these “physical” experiments, the models developed were used to carry out a program of “numerical” experiments, which provides a comprehensive database, allowing engineers and scientists to make proposals for improving or renewing standards.

#### 1.3.1. *MEFISTO* research program

In parallel with the CEOS.fr project, the Agence National pour la Recherche (ANR) launched the MEFISTO research project in 2008. As a result of the collaboration between the researchers’ teams of MEFISTO and CEOS.fr projects, it was possible to develop models, which consider the following topics and approaches:

- modeling of effects under monotonic loading in connection with the overall performance of the material (stress-strain model) and the local damage process (trajectory and width of cracks);

– modeling of THM-coupled effects on concrete at an early age and assessment of induced stresses and local damage.

The MEFISTO project also provided support to the CEOS.fr project for the design and construction of the full and 1/3-scale test bodies.

The development of numerical tools has provided an improved assessment of the macro-crack positions and crack openings, using post-processing tools for finite-element-based simulations (2D or 3D) and simplified approaches, such as multi-fiber beam models (based on 1D models).

### *Discrete and mixed methods*

Due to the joint use of continuous and discrete approaches, mixed approaches allow the simulation of the cracking pattern at the center of the model. The challenge posed by this approach is to allow the two models to coexist in the same calculation processing in parallel.

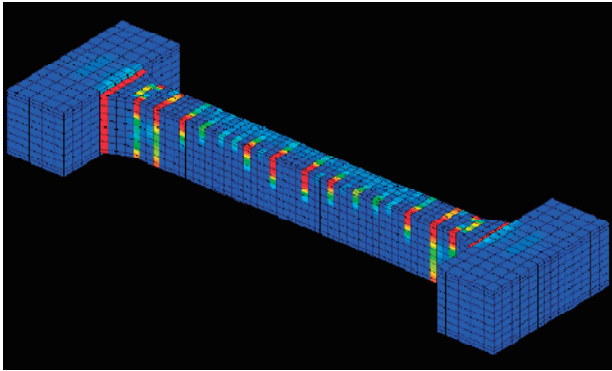


**Figure 1.19.** *Continuous method: cracking pattern of a restrained beam under early age shrinkage [SEL 14]*

In addition to these two approaches, special attention must be paid to consider the uncertainties associated with the prediction of crack opening and spacing. Reliability tools have been developed to be coupled with mechanical models. The difficulties associated with model coupling and computation run times are key points which require improvement for the future use of these tools on industrial applications.

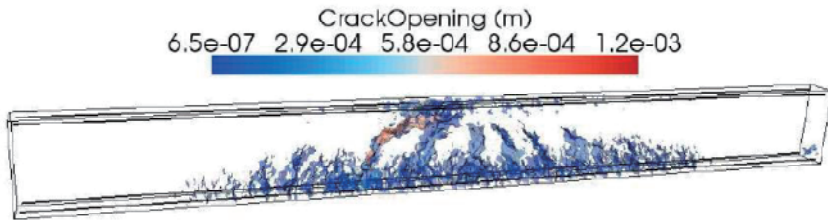


**Figure 1.20.** Cracking pattern on a 3-point bending R.C. beam resulting from the use of a mixed method [OLI 15]

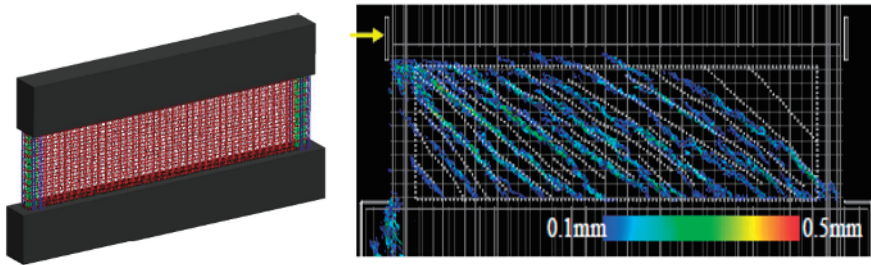


**Figure 1.21.** Cracking pattern for SHW3 test using discrete elements method [YAM 14]

### 1.3.2. Benchmarks and workshops

Following international benchmarking, a first workshop on the control of cracking in reinforced concrete structure – ConCrack1 – was held in December 2009. This promoted new relationships and increased exchange of information with the international scientific community. The performance of existing models was evaluated and compared to test results from the existing experiments. During this workshop, researchers presented the available modeling tools and exchanged their know-how. As a conclusion of the workshop, it was decided, based on the experiments derived from the CEOS.fr project, to organize an international benchmark exercise with the modeling of the behavior of the test mock-ups and large test bodies. The following were considered for the benchmark test: RL1 – large beam loaded in flexion with free shrinkage, RG8 – large beam with restrained shrinkage, and SHW3 – 1/3 scale shear wall under cyclic loading. A restitution workshop – ConCrack2 – was held in June 2011 and the main results were published in a special issue of the EJECE journal (September 2014).

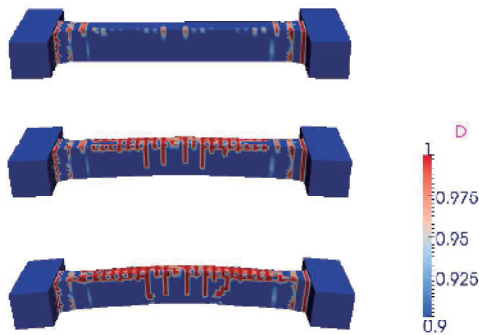


**Figure 1.22.** *Cracking evolution upon bending after restrained shrinkage operated on the beam RG8 (ConCrack2, Schreffler, Sciumé, Pesavento University of Padova)*

On the same theme, a further French-Japanese workshop – ConCrack 3 – was co-organized on THM effects in March 2012.

In March 2014, a final workshop – ConCrack 4 – co-sponsored by the European Joint Research Centre was held in Ispra (Italy). The main results obtained during the CEOS.fr program and related civil works in Europe were presented. Based on the results presented, standard rules for reinforced concrete, as applied to special structures, were proposed to a panel of international experts. In conclusion, it was decided to issue “Guidelines for the control of cracking in reinforced concrete structures”.

### 1.3.3. Numerical experiments

The numerical simulations performed showed that the models are able to adequately represent the behavior of the test specimens (static, cyclic and thermo-hydro-mechanical loads). It was decided to use these models to extend the experimental program through numerical experimental models.

A numerical simulation program was planned to supplement the results obtained from physical experiments, which analyze the effects of various parameters on cracking phenomena.

In particular, the effects of geometry, concrete cover, reinforcement ratio, concrete strength, etc. were studied.



Figure 1.23 gives an example of the impact of two different reinforcement ratios on crack occurrence under restrained shrinkage.

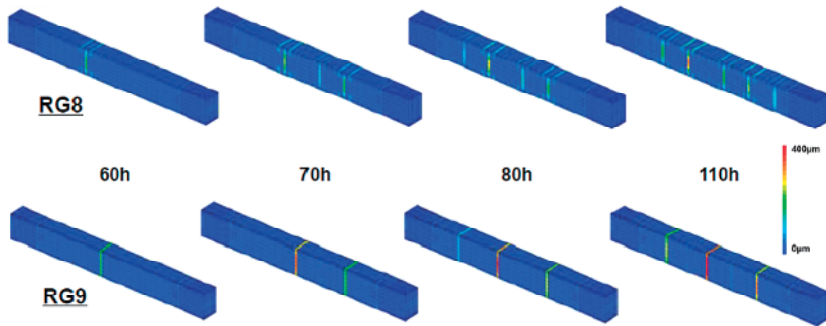


**Figure 1.23.** Coupled thermo-hydro-mechanical modeling to forecast the onset of cracking at early age under the effect of a restrained shrinkage for two beams to different ratios of reinforcement [SEL 14]

## 1.4. Engineering

In addition to the above data from tests on large bodies and modeling simulation, other results and data were used to support the CEOS.fr project, including:

- tests performed in laboratories (EPFL tests, Durham University tests) were used for the comparison with the results given by EC2 and MC2010 formulae dedicated to crack width and crack spacing calculation;

- for long-term results related to drying shrinkage and creep, a review of in-service measurement data from the monitoring and visual checks of existing structures has been used to supplement the above CEOS.fr test results. This data has been sourced from feedback from in-service structures: cooling towers, nuclear power plants (NPP), containments and associated large-scale models, such as the MAEVA model for NPP inner containment, concrete nuclear waste containers, cantilever prestressed decks and bridge piers.

Through the use of CEOS.fr project test and simulation results, complemented by test laboratory results and other inputs from the existing structures, the participants of the CEOS.fr project have formulated

engineering proposals to supplement the EC2 and MC2010 formulae. These proposals are presented in the following chapters.

## **1.5. Database and specimen storage**

### **1.5.1. Database CHEOPS**

Data related to the CEOS.fr project have been captured on an experimental and numerical database, CHEOPS, developed by the Numerical Engineering & Consulting Society, NECS (necs.fr).

The data are selected for the use of numerical benchmarking. They are presented in the form of experimental identification data sheets (FIDEX). Each data sheet provides the following information:

- summary;
- geometrical and technical characteristics (formwork setup and concrete reinforcement);
- material properties (test results and value data sheet);
- experimental procedures (test bench, environmental conditions and photos);
- measurements (description, sensors, patterns, numerical files, comments and analysis).

As a registered user, the database can be publicly accessed at the following website: <https://cheops.necs.fr/>

### **1.5.2. Specimen storage (Renardières site)**

Following testing, the RL and RG blocks have been stored by EDF on the Renardières Site located near Fontainebleau, France.